

THERMAL CONDUCTIVITY OF SYNTHETIC DIAMOND FILMS

C. P. BEETZ, Jr.*, T. A. PERRY, and D. T. MORELLI

Physics Department, General Motors Research Laboratories, Warren, Michigan 48090-9055, U.S.A.

The thermal conductivity of diamond films grown by hot filament assisted CVD has been measured over the temperature range 10K–300K. The thermal conductivity at room temperature is of the order 10 W/cm K and decreases monotonically with decreasing temperature. Since the films consist of microcrystallites of dimensions on the order of 2 μm , boundary scattering of phonons is expected to be large. The effect of boundary scattering on the lattice thermal conductivity is calculated and is in qualitative agreement with the observed results above about 30K. However, below this temperature, the measured conductivity shows an enhancement above that expected for boundary scattering alone. Using the Debye formulation for the thermal conductivity, the film crystallite size can be estimated as well as the concentration of point defects. Both the estimated crystallite size and the concentration of point defects is in good agreement with SEM observations and with hydrogen concentrations measured using elastic recoil detection. It is proposed that bond angle disorder present in the lattice can account for this unusual behavior.

1. Introduction

The use of diamond as a technologically important material has been hindered by the difficulty encountered in its synthesis, which is limited to producing relatively small crystals and powders. Over the past decade, the situation has changed to a large degree as workers have explored new and innovative ways to synthesize diamond. In particular, a great deal of attention has been focused on growing diamond using far from equilibrium thin film growth techniques. Recent developments using plasma, ion beam or hot filament assisted chemical vapor deposition techniques¹⁾ have created the potential for a wide variety of applications for diamond in areas as diverse as cutting tool coatings and high-temperature electronic devices.

There are many outstanding questions with regard to the physical properties of diamond films; in this paper we attempt to address the following two questions: (1) how well do diamond films conduct heat in comparison to natural diamond? and (2) how do changes in the growth conditions influence their ability to conduct heat? In this report we present the results of experiments on the

heat conduction properties of diamond films grown by hot filament assisted CVD for two different growth conditions. We also correlate the results of thermal conductivity, Raman and elastic recoil detection (ERD) measurements to give an insight into the type of defect structures present in diamond thin films grown by hot filament assisted CVD.

2. Experimental

The diamond films investigated in this research were grown at reduced pressure (~ 9.0 Torr) from dilute mixtures of methane (~ 0.18 – 1.00%) in hydrogen using hot filament assisted CVD at temperatures in the range of 650–1150°C. Details of the growth technique and sample analysis are presented elsewhere²⁾. The resulting films grew at rates of approximately 0.3–1.0 μmhr^{-1} depending on the methane concentration. The growth conditions for the films discussed in this report are summarized in Table I. The films were characterized using scanning electron microscopy, X-ray diffraction and Raman spectroscopy. A typical X-ray diffraction pattern taken with a Seeman-Bolin thin film diffractometer shows three sharp lines which can be indexed to a diamond cubic lattice as the $\langle 111 \rangle$, $\langle 220 \rangle$ and $\langle 311 \rangle$ reflections. The average

*Present address, Advanced Technology Materials, 520-B Danbury Rd., New Milford, CT 06776, U.S.A.

conductivity of the films is smaller than that of the single crystal diamond everywhere throughout the temperature range studied. Below room temperature, the thermal conductivity decreases faster than T^2 down to about 30°K. At 30°K there is a “knee” in the thermal conductivity below which the temperature dependence is much weaker.

It is not surprising that the magnitude of κ is smaller and that the peak in $\kappa(T)$ is shifted toward higher temperatures relative to “bulk” single crystal diamond, since the films are polycrystalline and consist of small crystallites of sizes on the order of a few microns. Boundary scattering alone leads to a T^3 dependence of $\kappa(T)$, a behavior closely followed in bulk diamond⁵⁾, and clearly in the diamond film data this temperature dependence is being approached below 100°K. The strong deviation from this temperature dependence below 30°K, leading to a large enhancement of κ over its boundary-limited value, is very surprising and not observed in natural crystals.

A more insightful approach to understanding film thermal conductivity is to fit the data using a standard Debye-type expression. The thermal conductivity of a crystal can be expressed as⁶⁾

$$\kappa(T) = (4\pi k^4 T^3 / \nu h^3) \int_0^{\theta/T} \tau(x) (x^4 e^x) dx / (e^x - 1)^2. \quad (2)$$

In this equation, k and h are the Boltzmann and Planck constants respectively, $x = h\omega/kT$ where ω is the phonon frequency, $\theta = 2230^\circ\text{K}$ is the Debye temperature⁷⁾, $\nu = 1.32 \times 10^4 \text{ ms}^{-1}$ is the averaged phonon velocity⁵⁾ and τ is the phonon scattering time. In general there is more than one type of scattering process acting on the phonons, and one must add the corresponding scattering rates to determine τ . For diamond we include scattering by crystal boundaries τ_b , other phonons via Umklapp processes τ_p and point defects such as isotopes and impurities in the lattice τ_i . The point defect term can be further separated into two components, a rate τ_{is}^{-1} due to ^{13}C isotopes in the lattice, and a rate τ_{im}^{-1} due to point defect scattering from other types of impurities (substitutional, interstitial and vacancy sites). This is done because even in the

purest Type IIa diamonds, ^{13}C isotopes are present at a naturally occurring level of about 1.1%. The U-process and isotope scattering terms for diamond take the forms⁸⁾

$$\tau_p^{-1} = 1.31 T^4 x^2 \exp(-270/T) \quad (3)$$

and

$$\tau_{is}^{-1} = 0.0346 x^4 T^4.$$

The boundary scattering rate takes the form⁶⁾

$$\tau_b(x)^{-1} = \nu / 1.12d, \quad (4)$$

where d the crystallite size is adjusted to give the best fit to the data. While for point defect scattering⁶⁾,

$$\tau_{im}^{-1} = I x^4 T^4. \quad (5)$$

Here I is an adjustable parameter used to fit the data, this term describes scattering by impurities (other than ^{13}C) and other point defects in the lattice. The total scattering rate is then given by

$$\tau(x)^{-1} = \tau_b^{-1} + \tau_p^{-1} + \tau_{is}^{-1} + \tau_{im}^{-1}. \quad (6)$$

The result of the fitting procedure is shown by the solid lines in Fig. 1; the data of reference 4 (dashed line) can be fit with $d = 1 \text{ mm}$ (which is the reported size of the crystal used in ref. 4) and $I = 0$. From the figure we see that decreasing d drives both the magnitude of κ down and shifts the peak to higher temperatures. For $d = 1.0 \text{ }\mu\text{m}$ the peak just begins to set in at 300°K. The value of d which gives the best fit to our data is $d = 1.5 \text{ }\mu\text{m}$, in reasonable agreement with the observed crystallite sizes in the films. The fit can be improved slightly by including an additional point defect term corresponding to $I = 0.045^\circ\text{K}^{-4}\text{s}^{-1}$, where I can be related to the concentration of point defects in the lattice by the expression⁶⁾

$$I = (c_{im} a^3 k^4 \Delta M^2) / (4\pi \nu^3 h^4 M^2). \quad (7)$$

Here c_{im} is the relative point defect concentration, a the nearest neighbor distance = 1.54 Å in diamond, M is the mass of a carbon atom and ΔM the

difference in mass of an impurity atom and a carbon atom. The most likely additional point defects in our films are vacancies or hydrogen atoms. For these defects, $\Delta M/M=1$ and 0.92 , and from the fitted value of I we find $c_{\text{im}}=0.0012$ (0.12%) and 0.0014 (0.14%), respectively. This is not an unreasonable number and is a likely explanation of the additional point defect scattering in our films.

We also show in Fig. 1 the results over the temperature range $200\text{--}300\text{ K}$ for a film that was grown at higher methane concentrations (0.99%). In this case the conductivity drops by approximately an order of magnitude and a fit of the data over this brief temperature range yields a crystallite size of $\sim 0.1\ \mu\text{m}$, in qualitative agreement with scanning electron micrographs which show a much smoother surface morphology.

Below 30 K the data diverges from the above fit; this is clearly seen in Fig. 1. In this temperature regime, the conductivity varies much more slowly than the T^3 dependence expected for boundary scattering. Specular reflection of phonons has

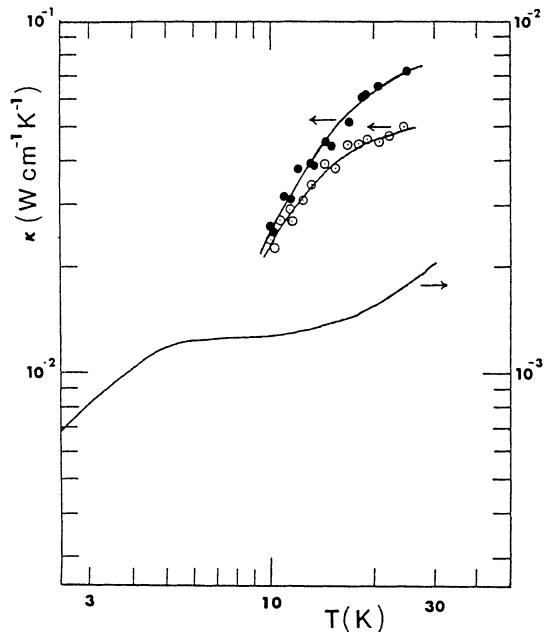


Fig. 2. Difference between measured thermal conductivity and that determined using the fitting routine described in the text. The solid line indicates the thermal conductivity of amorphous SiO_2 .

been observed to slow the temperature dependence of κ in diamond at low temperatures, but it is unlikely that this mechanism can account for the magnitude of the effect observed here. We propose that this behavior is due to a small amount of disordered carbon in the lattice.

In Fig. 2 we plot the difference between the measured conductivity and that determined by the above fit in order to test this hypothesis. The difference conductivity shows a plateau-like behavior above 15 K and falls off below this tempera-

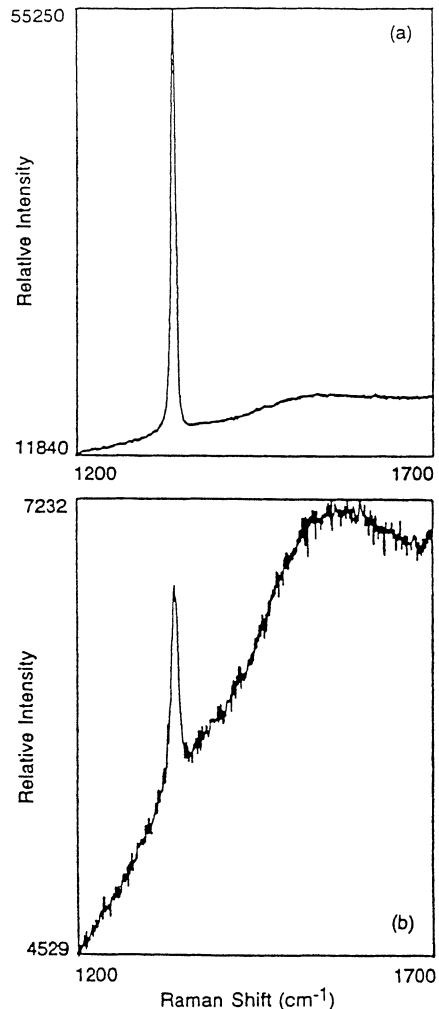


Fig. 3. The unpolarized room temperature Raman spectrum of films DT-22 and DT-23. Note the difference in relative intensities of the 1332 cm^{-1} and 1580 cm^{-1} features. The sloping backgrounds in both spectra are due to an underlying photoluminescence feature.

ture. This is reminiscent of the thermal conductivity of many amorphous systems such as SiO₂, also shown in Fig. 2. The magnitude of this contribution (~ 0.02 W/cm² K at 10° K) as well as the plateau temperature ($\sim 20^\circ$ K) are both higher than those of typical amorphous systems. However, this is consistent with Freeman and Anderson's model⁹⁾, in which both of these parameters are shown to scale with the Debye temperature of the amorphous system.

Thus we believe that the weak temperature dependence that we observe in our films below 30° K is due to the presence of a small amount of disordered material in the lattice. This is further substantiated by Raman scattering studies (Fig. 3) which reveal a broad peak near 1580 cm⁻¹ in addition to the diamond phonon at 1334 cm⁻¹. The presence of the 1580 cm⁻¹ peak is indicative of the presence of bond angle disorder induced by incorporating sp² hybridized carbon into the primarily sp³ lattice¹⁰⁾. This result is also in agreement with the results of ERD measurements¹¹⁾ which show that there is an underlying hydrogen content on the order of ~ 0.1 atomic percent in films grown at relatively low methane concentrations (0.18%) and this could give rise to the effects observed in the Raman spectra. The ERD analysis of films grown at 0.99% methane yield hydrogen concentrations of ~ 0.2 atomic percent below the film surface. These results point to a general trend that as the methane concentration in the growth gas increases, the hydrogen concentration of the films increase. This observation is consistent with the results of Raman scattering (Fig. 3) which also show an increase in the scattering intensity in the

1580 cm⁻¹ region with increasing methane concentration. We propose that the Raman scattering intensity observed at ~ 1580 cm⁻¹ is due to the presence of bond angle disorder effects induced by the presence of a significant amount of hydrogen in the bulk of the film, and that this scattered intensity increases with increasing methane concentration in the film.

Acknowledgements. We would like to thank J. P. Heremans for many useful comments and critical reading of the manuscript and B. M. Clemens for the use of the X-ray diffractometer.

REFERENCES

- 1) R. C. DeVries, *Annual Rev. Mat. Sci.* **17**, 161 (1987) and references cited therein.
- 2) C. P. Beetz and T. A. Perry, General Motors Research Publication GMR-6093.
- 3) P. Villars and L. D. Calvert, *Pearson's Handbook of Crystallographic Data or Intermetallic Phases*, Vol. 2, 1500 (1985) Amer. Soc. for Metals, Metals Park, Ohio.
- 4) R. Berman, E. L. Foster, and J. M. Ziman, *Proc. R. Soc. London, Ser. A* **237**, 344 (1956).
- 5) J. W. Vandersande, *Phys. Rev. B* **13**, 4560 (1976).
- 6) R. Berman, *Thermal Conduction in Solids*, Clarendon, Oxford, 1976.
- 7) D. L. Burke and S. A. Friedberg, *Phys. Rev.* **111**, 1275 (1958).
- 8) V. I. Nepsha, N. F. Reshetnikov, Yu. A. Klyuev, G. B. Bokii, and Yu. A. Pavlov, *Sov. Phys. Dokl.* **30**, 547 (1985).
- 9) J. J. Freeman and A. C. Anderson, *Phys. Rev. B* **34**, 5684 (1986).
- 10) D. Beeman, J. Silverman, R. Lynds, and M. R. Anderson, *Phys. Rev. B* **30**, 870 (1984).
- 11) T. A. Perry and C. P. Beetz, Jr., General Motors Research Publication GMR-6370.